CFD Letters

A Comparative Study on Hydrodynamic Analysis with and without Cavitation Modelling: A Study on Textured Slip Journal Bearing

Althesa Androva[1, 3,*], Muhammad Tauviqirrahman[1], Nazaruddin Sinaga[1], Muhammad Khafidh[2], Muhammad Sagaf[1,4], Hafid[5]

1   Department of Mechanical Engineering, Faculty of Engineering, Diponegoro University, Semarang, Indonesia
2   Department of Mechanical Engineering, Faculty of Industrial Technology, Universitas Islam Indonesia,Yogyakarta, Indonesia
3   Deparment of Mechanical Engineering, Faculty of Engineering and informatic, Universitas PGRI Semarang, Indonesia
4   Department of industrial Engineering , Faculty of Industrial Technology, Universitas Islam Sultan Agung, Semarang, Indonesia
5   Research Center for Testing Technology and Standards (PRTPS), National Research and Innovation Agency (BRIN), Indonesia

ARTICLE INFO	ABSTRACT
  	In journal bearing modeling, the phenomenon of cavitation is very important to improve the accuracy of the simulation results. This is because cavitation will almost certainly occur because there are convergent and divergent geometries. The results of the simulation will be close to real conditions so that it can have a positive effect on researchers in order to design optimal journal bearings. The effect of modeling without cavitation and with cavitation on journal bearing modeling has a great influence on the lubrication performance of journal bearings. In modeling with cavitation, the maximum hydrodynamic pressure and load carrying capacity that the journal bearing is capable of relying on has a fairly rapid increase. The modeling results also relate to the friction force that occurs in the journal bearing. The aim of the present study is to explore the effect of inclusion of modeling of the Hydrodynamic pressure. The finite volume method based on software is used to compare the result with and without cavitation. Here, The mixture multiphase cavitation is adopted. The numerical result show the effect of modelling without cavitation and with cavitation on journal bearing modelling has a great influence on the lubrication performance of journal bearings. In modelling with cavitation, the maximum hydrodynamic pressure and load cmarrying capacity that the journal bearing is capable of relying on has a fairly rapid increase. The modelling results also relate to the friction force that occurs in the journal bearing.

1. Introduction

Until now, journal bearings are used as indispensable bearings in many rotating machines such as steam turbines, generators, blowers, compressors, thoracic machines and so on. This is because journal bearings are superior to other bearings in vibration resistance, stability, and long service life.

---

* Corresponding author.
E-mail address: androthesa@gmail.com (Althesa Androva)

All these characteristics come from the principle of journal bearings that support the shaft with a thin oil film. In addition, the smaller outer diameter of the journal bearing compared to other bearings is often an advantage for the designer of a machine [1].

Industry activists are currently facing pressure to reduce energy consumption in order to protect the environment, and can increase the service life of a component to reduce production costs. The rapidly increasing industry development and human needs expose scientists to the problem of being able to create journal bearings with a minimum design, but still able to provide maximum performance. Various methods have been proposed by various scientists to improve the performance of journal bearings. The suitable condition of textured journal bearing needs to be chosen correctly to optimize the maximum film pressure of journal bearing load and load-carrying capacity of journal bearing [2]. One of the commonly used methods is to perform surface engineering in the form of providing slip / no-slip boundary conditions and textures on the surface of the journal bearing.

The effect of designed slip on the noise produced by thrust bearings study, demonstrate how incorporating slip can reduce noise levels, turbulence kinetic energy (TKE), and turbulence eddy dissipation (TED) rate. At high film thickness, the average APL, TKE, and TED values were the lowest [3].

Sliding bearings tolerate direct loading. In contrast to roller element bearings, which have a roll or ball between the inner and outer rings. The sliding bearing contact mechanism is a sliding operation that takes place on the contact surface between the rotating and fixed elements [4].

When operating at specified external loads, as the load-carrying capacity diminishes, so does the thickness of the film, which tends to raise the shear rate and then friction. Thus, in the case of uniform slip conditions, the gain from shear decrease in friction is negated by increased shear rate produced by film thickness reduction [5].

The provision of slips generally causes a decrease in friction force, so it can be used to create a journal bearing design with a low friction force. However, if slip is applied to the entire surface of the bearing, it can reduce the load carrying capacity of the journal bearing. When operating at a specified external load, if the load carrying capacity decreases, the film thickness will be thinned, tending to increase friction

Journal bearings with surface modification by means of texture can improve hydrodynamic performance because they can reduce friction. Different surface shapes can create different flow patterns in the journal bearing. Differences in topographic patterns due to surface texture provide a micro-reservoir effect for lubrication fluids and micro-traps for metal debris due to wear that occurs in journal bearings. [6]. The hydrophobic coating has a significant impact on fluid behavior, particularly load-carrying ability. A hydrophobic coating can increase the performance of a journal bearing [7]. However, the provision of surface texture causes changes in the thickness of the lubrication fluid which can have a direct impact on changes in the pressure and load carrying capacity of the journal bearing, so it is necessary to pay attention to the selection of the right surface texture parameters in order to obtain optimal journal bearing performance. Computational Fluid Dynamics (CFD) is a system study that uses computer-based simulations to analyze fluid flow, heat transfer, and other fluid phenomena such as chemical reactions. CFD analysis techniques are powerful and have several applications in both industry and non-industrial settings. For instance, in aircraft aerodynamics, ship hydrodynamics, turbine flow, and so on [8].

1.1 Theory

Fluid mechanics equations, which have been known for over a century, can only be solved for a restricted number of flows. The known solutions are tremendously valuable in understanding fluid movement, but they are rarely directly applicable in engineering analysis or design. Engineers have historically been required to employ other methods. The most popular strategy employs equation simplifications. These are often based on a combination of approximations and dimensional analysis, with virtually always some empirical input required [9].

Surface texture is an identical characteristic on a surface that is purposefully well-identified. Surface roughness, in contrast to texture, is often random and difficult to identify [10].

1.1.1 Navier stoke

Based on the work principle of the journal bearing, two sliding surfaces are necessary for the formation of the bearing lubrication. The Navier-Stokes and continuity equations are used to solve the lubrication problem according to a finite-volume method [11].

The Reynolds-averaged Navier-Stokes (RANS) equations, in particular, are used to obtain the hydrodynamic lubrication pressure in order to quantify the bearing noise caused by the lubricant. It should be noted that the Reynolds decomposition, which includes the breakdown of an instantaneous quantity into its time-averaged and fluctuating components, is the primary technique for deriving the RANS equations from the instantaneous Navier-Stokes equations. The separation of a variable (such as velocity u) into its mean (time-averaged) component ($\bar{u}$) and its fluctuating component (u') is referred to as Reynolds decomposition [12]. The expressions for the continuity equation and the RANS equation are as follows.

$$\frac{\partial}{\partial x_i}\left(\rho u_i u_j\right)^n = -\frac{\partial p}{\partial x_i} + \frac{\partial}{\partial x_j}\left[\mu\left(\frac{\partial u_i}{\partial x_j} + \frac{\partial u_j}{\partial x_i}\right)\right] + \frac{\partial}{\partial x_j}\left(-\rho u_i' u_j'\right) \tag{1}$$

The standard turbulent kinetic energy and turbulent dissipation rate, whose definitions are expressed below:

$$k = \frac{u_i' u_j'}{2} \text{ and } \varepsilon_d = \frac{\mu}{\rho}\left(\frac{\partial u_i'}{\partial x_j}\frac{\partial u_i'}{\partial x_j}\right) \tag{2}$$

The most used slip model is the slip length model. Navier [13] proposed this model, which states that the slip speed is directly proportional to the shear rate at the interface. To forecast Interface slip speed, the model use a length parameter known as slip length, written as:

$$\mathcal{V}_s = \alpha \dot{\gamma} \tag{3}$$

The lubricant has a critical shear stress, and a new slip state will emerge when the shear stress in the boundary layer between the fluid and the solid surface wall is high enough [14].

1.1.2 Cavitation

When the textured surface is applied to the bearing, cavitation may develop, lowering or enhancing lubrication performance depending on the texturing settings. Because cavitation has a

substantial impact on hydrodynamic pressure, the cavitation model should be incorporated in the analysis [15].

The majority of the research presumes perfect conditions with negative tension in the lubricating layer. Only a minority of the literature, according to Shi and Ni [16] predicts the existence of cavitation when the pressure in the fluid layer declines at a given rate. In general, the cavitation mechanism consists of two components:

i. When the pressure falls below atmospheric pressure, the ability of air to dissolve in the fluid reduces, causing air to form cavitation on the fluid layer.
ii. When the lubricant pressure falls below the saturated vapor pressure, the phase transition from liquid to vapor occurs.

Cavitation has a large impact on load support and frictional performance. As a result, when investigating the influence of bearing surface texture, the effects of cavitation are also considered [17].

The effect of cavitation on the hydrodynamic performance of textured surfaces is investigated, and it is also proposed that cavitation has a major effect on performance near parallel surfaces [18].

The Schnerr-Sauer cavitation model is used to mass transfer via the vapor phase and liquid phase interfaces, using a combination of water and vapour that contains a large number of spherical vapour mixtures to mimic the processes of evaporation and condensation, respectively [19].

In cavitation, the vapor transport equation governs the liquid-vapor mass transfer (evaporation and condensation). It says:

$$\frac{\partial}{\partial t}(\alpha_V \rho_v) + \nabla \cdot (\alpha_V \rho_v \, V) = R_e - R_c \tag{4}$$

To account for the cavitation effect, a model presented by Zwart-Gerber-Belamri [20] is used, in which all bubbles in the system are assumed to be the same size. To account for the phase shift rates during vapor generation and condensation, Zwart-GerberBelamri developed the following formulations based on generalized Rayleigh-Plesset equations.

If $P \leq P_v$

$$R_e = F_v \frac{3_{anuc}(1 - \alpha_v)\rho_v}{R_B} \sqrt{\frac{2(P_V - P)}{3\rho}} \tag{5}$$

If $P \geq P_v$

$$R_c = F_{cond} \frac{3\alpha\rho_v}{R_B} \sqrt{\frac{2(P - P_V)}{3\rho}} \tag{6}$$

Where p_v is the vapor pressure, F_v is the evaporation coefficient, and F_{cond} is the condensation coefficient.

2. Methodology

The journal bearing consists of a shaft that rotates relative to the housing as can be seen in Figure 1 below. Lubrication fluid fills the gap between the two surfaces to prevent lubrication failure in the journal bearing. The thickness of the lubrication fluid film that separates the two surfaces is a function of the following equation 2.3:

$$h(\theta) = c(1 + \varepsilon \cos \theta) \tag{7}$$

Where h (θ) is the height of the fluid at an angle of θ, c is the radial clearance i.e. the difference between the shaft radius and the housing radius, and ε is the ratio of eccentricity to the radial clearance journal bearing.
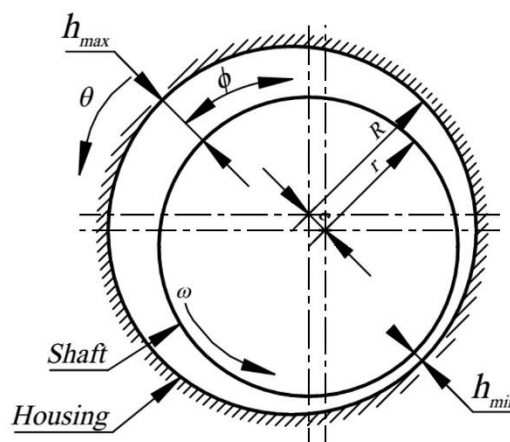
Fig. 1. Journal bearing schema

The geometry of the journal bearings used in simulating various cases of fluid flow of journal bearings in this research adopts Cupillard's proprietary journal bearing geometry [21] with the geometric characteristics of the journal bearing and the characteristics of the lubricating fluid as follows (see Table 1).

Table 1
Geometric characteristics of the journal bearing and the characteristics of the lubricating fluid

Bearing width	L_y = 100 mm
Shaft radius	r = 50 mm
Hausing radius	R = 50.145 mm
Radial clearance	c = 0.145 mm
Eccentricity ratio	ε = 0.2, 0.5, dan 0.8
Eccentricity	$e = \varepsilon . c = 0.2 \ (0.145) = 0.0290 \ mm$
	$e = \varepsilon . c = 0.5 \ (0.145) = 0.0725 \ mm$
	$e = \varepsilon . c = 0.8 \ (0.145) = 0.1160 \ mm$
Lubricant density	ρ = 840 kg/m^3
Lubricant viscosity	η = 0.0127 Pa.s
Vapour density	ρ = 1.2 kg/m^3
Vapour viskosity	η = 2x10^{-5} Pa.s
Saturated pressure	20,000 Pa
Shaft rotational speed	ω = 48.1 rad/s

Although in real conditions the journal bearing has a defined length value in its axial direction, in this research the journal bearing will be modeled as an infinitely wide journal bearing. In this case the width of the journal bearing in the axial direction will be neglected, as will the leakage on the side of the journal bearing (side leakage). Because the ratio of the thickness of the lubricating fluid film to the shaft radius is very small, the curvature of the lubricating fluid film can be neglected. Thus, the lubricating fluid from the journal bearing can be modeled as a graph of the cosine function as shown in Figure 2 below. The housing section is modeled as a stationary profile with a wavelength of , while the shaft is modeled as a flat surface moving with a velocity [22].
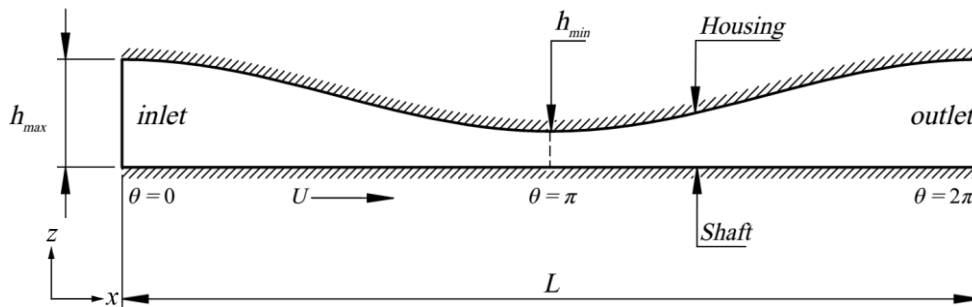
Fig. 2. Simplification of fluid domain infinitely wide journal bearings

Before verifying the case, an independent grid analysis of the geometric modeling must be performed to demonstrate that the findings generated from this geometric modeling are no longer influenced by the mesh employed. Independent grid studies are performed by altering the number of grids in both the horizontal (Nx) and vertical (Ny) directions, and then comparing the findings to the reference results.

As seen in Figure 3, Pmax begins to stabilize when the number of components exceeds 60,000, as indicated by lines on the graph that become more linear as the number of elements increases. As a result, the meshing employed is stated to be independent and capable of being used in simulation. As a result, the number of elements employed in this simulation is 100,000 because it produces the most stable results.
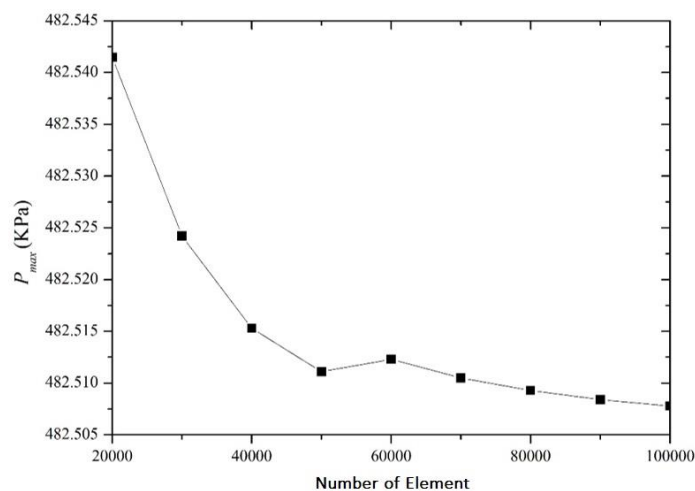
Fig. 3. Grid independence journal bearing graphics

2.1 Validation

Journal Bearing with Multitextured Groove and No-Slip Boundary Conditions

This case will explain the effect of giving multitextured grooves and no-slip boundary conditions on one of the journal bearing surfaces on the lubrication performance of the journal bearing.

The pressure distribution derived from the current study simulation follows the same trend as the results of the Cupillard simulation (2008) [21], as shown in Figure 4. The area of cavitation that occurred in the current study simulation and Cupillard (2008) is nearly same.
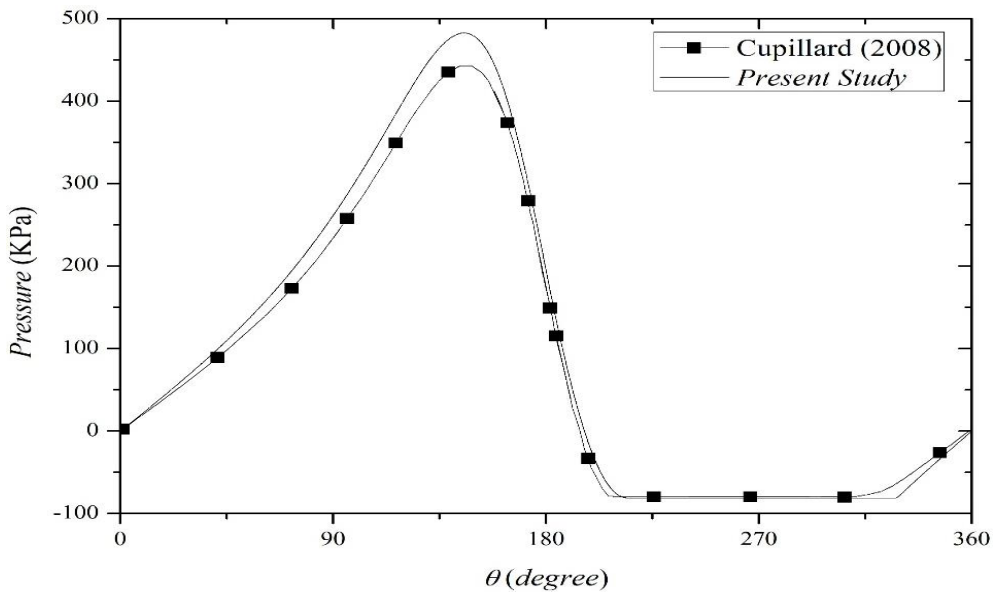
Fig. 4. Cupillard (2008) and the current study's journal bearing pressure distribution

In this case, the multi-textured groove is only applied to the converging portion of the journal bearing housing surface. The geometry of the journal bearing used in this case can be seen in Figure 5 with a simplified geometry of the journal bearing and the geometry of one cell with elementary groove texture as shown in Figure 6 below. See Table 2 for Journal bearing geometry specification.
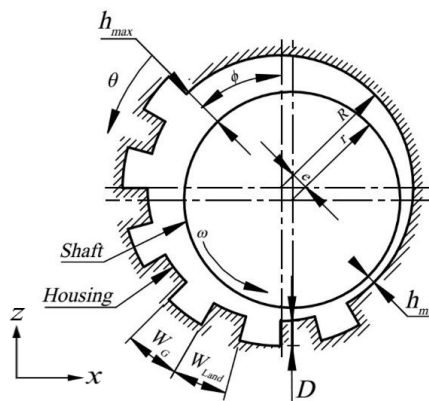
Fig. 5. Geometry of journal bearings with multiple groove textures and no slip boundary conditions
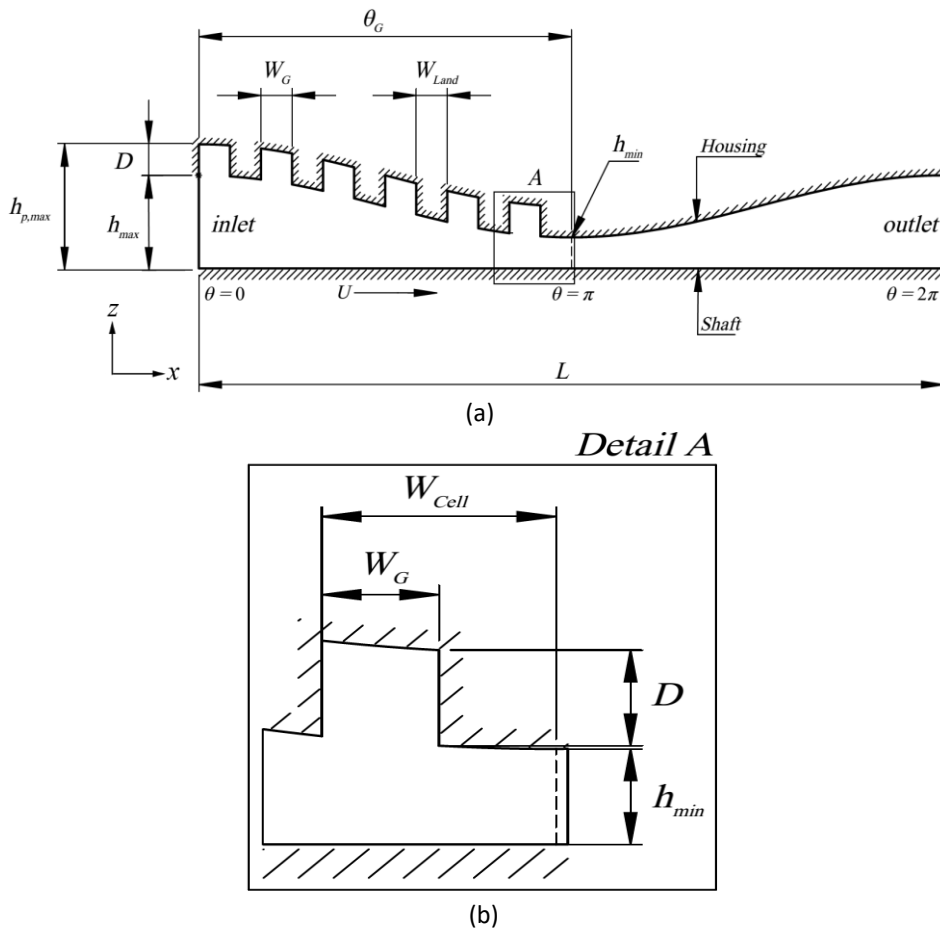
Fig. 6. (a) Simplified journal bearing geometry modeling (b) Geometry of one cell elementary groove texture

Because the fluid flow modeling carried out in this study is an incompressible fluid flow model with a low fluid flow rate, a pressure based solver with the COUPLED algorithm will be used to solve all case simulations in this study. Because the fluid flow modeling carried out in this study is an incompressible fluid flow model with a low fluid flow rate, a pressure based solver with the COUPLED algorithm will be used to solve all case simulations in this study.

- Determination of the Solution Method

The spatial discretization for gradient, pressure, and momentum in this study uses least square cell based Gradient, PRESTO pressure, QUICK momentum, QUICK volume fraction, QUICK turbulent kinetic energy, and QUICK turbulent dissipation rate because it provides fast but accurate simulation results compared to other discretization.

The next stage is to determine the Under Relaxation Factor (URF) to control the solutions from the simulations carried out. Under relaxation factors are used in numerical computations to stabilize and improve the convergence of numerical schemes involving iterative procedures. Although theoretically changing the value of the under relaxation factor will not affect the final result of the simulation, changing the under relaxation factor can increase the time of the numerical computations being performed. Therefore, in this final project, the default value of the recommended under relaxation factor is used.

Table 2
Journal bearing geometry specification (in mm)

Parameters	Symbol	Ecentricity ratio (ε)		
		0.2	0.5	0.8
Regional curve equation without texture	γ	$\gamma = 0.0290.\cos\left(\frac{200_x}{10029}\right) + 0.145$	$\gamma = 0.0725.\cos\left(\frac{200_x}{10029}\right) + 0.145$	$\gamma = 0.1160.\cos\left(\frac{200_x}{10029}\right) + 0.145$
Maximum fluid thickness	h_{max}	0.1740	0.2175	0.2610
Minimum fluid thickness	h_{min}	0.1160	0.0725	0.0290
Textured surface area length	θ_G	30º 60º 90º 120º 150º 180º	30º 60º 90º 120º 150º 180º	30º 60º 90º 120º 150º 180º
One groove texture unit length	W_G	5º	5º	5º
The length of the gap between textures	W_{Land}	5º	5º	5º
One texture cell unit length	W_{Cell}	10º	10º	10º
Wavelength	L	100.29π	100.29π	100.29π
Texture density	ρ_T	0.5	0.5	0.5
Texture depth ratio	D/h_{min}	0.5 1.0 1.5	0.5 1.0 1.5	0.5 1.0 1.5
Texture aspect ratio	λ	5º / (0.5h_{min}) 5º / (1.0h_{min}) 5º / (1.5h_{min})	5º / (0.5h_{min}) 5º / (1.0h_{min}) 5º / (1.5h_{min})	5º / (0.5h_{min}) 5º / (1.0h_{min}) 5º / (1.5h_{min})

To improve the accuracy of the fluid flow simulation results, it is necessary to set the convergence value limits of the iterations carried out. By default, the convergence value is set at a residual value limit of 10-3. Although in general this value is sufficient to represent the simulated fluid flow shape, if the simulation results obtained have not reached an acceptable limit value, then the convergence limit value can be lowered. In this simulation, the limit value of convergence 10^{-4} is used.

- Post Processing

At this stage data processing is carried out, where the raw data resulting from the iteration process is processed into plots, contours and vectors as can be seen in Figure 7 below so that it can be easily understood.
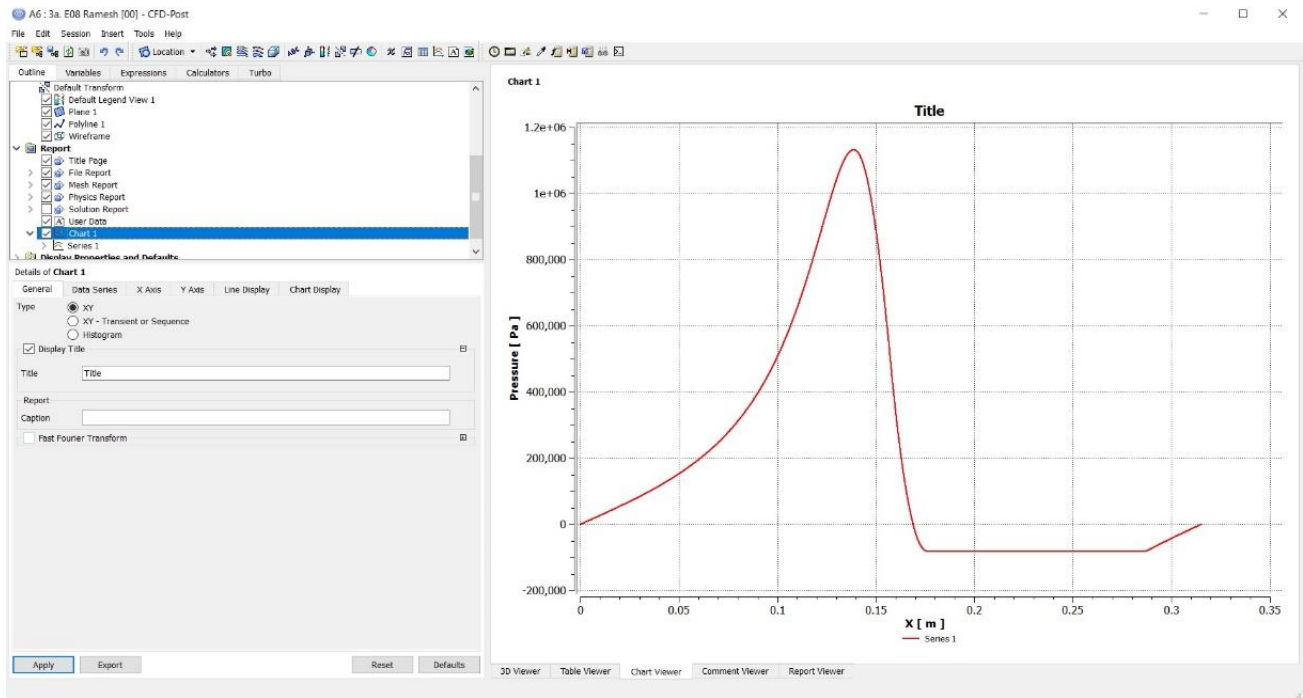
Fig. 7. Making a graphical plot of pressure distribution on a journal bearing

3. Result

3.1 Effect of ε Ratio

Based on table 3, Cavitation has a significant impact on journal bearing performance, with ε = 0.2 at all texture ratios. Journal bearings' maximum pressure and load bearing capacity have increased. When the hydrodynamic pressure falls below the cavitation pressure in the simulation of journal bearings with cavitation, the journal bearing loses hydrodynamic pressure due to the change in phase of the lubricant fluid from liquid to vapour in the diverging zone. The presence of straight lines in the diverging geometry of journal bearings distinguishes it. However, as it approaches the entrance area, the cavitation will vanish and the hydrodynamic pressure will gradually rise again. However, the frictional force in cavitation simulations has increased when compared to non-cavitation simulations.

Based on table 4, Cavitation has a significant impact on journal bearing performance, with ε = 0.5 at all texture ratios. Journal bearings' maximum pressure and load bearing capacity have increased. When the hydrodynamic pressure falls below the cavitation pressure in the simulation of journal bearings with cavitation, the journal bearing loses hydrodynamic pressure due to the change in phase of the lubricant fluid from liquid to vapour in the diverging zone. The presence of straight lines in the diverging geometry of journal bearings distinguishes it. However, as it approaches the entrance area, the cavitation will vanish and the hydrodynamic pressure will gradually rise again. However, the frictional force in cavitation simulations has increased when compared to non-cavitation simulations.

Based on table 5, Cavitation has a significant impact on journal bearing performance, with ε = 0.8 at all texture ratios. Journal bearings' maximum pressure and load bearing capacity have increased. When the hydrodynamic pressure falls below the cavitation pressure in the simulation of journal bearings with cavitation, the journal bearing loses hydrodynamic pressure due to the change in phase of the lubricant fluid from liquid to vapour in the diverging zone. The presence of straight lines in the diverging geometry of journal bearings distinguishes it. However, as it approaches the entrance area, the cavitation will vanish and the hydrodynamic pressure will gradually rise again. However, the frictional force in cavitation simulations has increased when compared to non-cavitation simulations.

Table 3
Simulation result of journal bearing with ε: 0.2 d/h 0.5, d/h: 1, and d/h: 1.5

D/h_{min}	ϑ	with cavitation			without cavitation		
		P_{max} (kPa)	W (kN)	F (N)	P_{max} (kPa)	W (kN)	F (N)
0.0	0º	87.11	-0.14	71.54	102.39	1.72	77.04
0.5	30º	88.52	0.12	71.65	103.42	1.88	76.99
	60º	92.41	0.55	71.66	107.23	2.25	76.99
	90º	98.02	1.33	71.51	112.39	2.83	76.90
	120º	111.17	2.63	71.16	126.25	3.76	76.67
	150º	109.41	4.21	70.46	122.75	4.73	76.16
	180º	98.72	5.44	69.20	110.22	5.93	74.93
1.0	30º	86.24	-0.30	71.61	100.77	1.40	76.88
	60º	87.80	-0.22	71.58	101.86	1.45	76.84
	90º	91.34	0.31	71.40	104.45	1.79	76.69
	120º	103.51	1.52	71.05	116.88	2.58	76.41
	150º	102.83	3.18	70.36	114.75	3.64	75.95
	180º	92.57	4.62	69.12	102.41	4.82	74.80
1.5	30º	84.05	-0.70	71.51	98.45	1.05	76.78
	60º	83.25	-0.99	71.38	97.02	0.73	76.59
	90º	84.19	-0.76	71.11	96.78	0.78	76.32
	120º	93.76	0.19	70.70	106.35	1.39	75.97
	150º	92.58	1.69	69.97	104.06	2.25	75.42
	180º	84.05	3.09	68.72	92.78	3.08	74.44

Table 4
Simulation result of journal bearing with ε: 0.5 d/h 0.5, d/h: 1, and d/h: 1.5

D/h_{min}	ϑ	without cavitation			with cavitation		
		P_{max} (kPa)	W (kN)	F (N)	$Pmax$ (kPa)	W (kN)	F (N)
0.0	0º	265.11	-0.07	101.33	337.71	21.53	96.27
0.5	30º	257.95	-0.70	101.17	328.53	20.63	95.90
	60º	254.86	-1.26	101.09	324.95	19.98	95.72
	90º	252.13	-1.87	101.22	321.10	19.38	95.66
	120º	252.56	-1.60	101.00	317.98	19.26	95.50
	150º	271.99	-0.10	100.73	342.90	20.13	95.42
	180º	248.63	2.54	99.81	315.38	20.67	93.89
1.0	30º	254.90	-1.23	101.02	324.93	20.04	95.70
	60º	248.30	-2.28	100.81	317.21	18.83	95.29
	90º	241.29	-3.36	100.81	308.12	17.69	95.03
	120º	297.25	-3.45	100.54	298.74	17.14	94.69
	150º	257.48	-1.95	100.23	320.44	17.86	94.58
	180º	234.67	1.24	99.31	294.92	18.65	93.23
1.5	30º	252.58	-1.63	100.88	322.22	19.59	95.50
	60º	243.28	-3.07	100.51	311.41	17.96	94.88
	90º	232.69	-4.54	100.36	298.30	16.42	94.40
	120º	224.11	-4.99	99.97	283.50	15.51	93.90
	150º	240.09	-3.75	99.61	298.80	15.97	93.63
	180º	219.87	-0.52	98.30	276.50	16.74	92.25

Table 5
Simulation result of journal bearing with ε: 0.8 d/h 0.5, d/h: 1, and d/h: 1.5

D/h_{min}	ϑ	without cavitation			with cavitation		
		P_{max} (kPa)	W (kN)	F (N)	P_{max} (kPa)	W (kN)	F (N)
0.0	0º	904.41	-0.57	188.67	1132.22	59.46	153.86
	30º	910.73	-0.38	189.20	1140.55	60.00	153.95
	60º	890.07	1.40	188.03	1120.85	60.26	152.69
0.5	90º	889.76	-0.82	188.19	1115.94	58.75	152.80
	120º	871.95	-0.71	187.36	1096.76	57.96	151.87
	150º	874.68	-3.38	188.11	1088.28	56.06	152.38
	180º	871.60	3.44	188.18	1119.99	58.58	150.47
	30º	908.90	-0.69	189.04	1138.35	59.62	153.74
	60º	885.67	0.74	187.66	1115.80	59.47	152.26
1.0	90º	880.57	-1.98	187.55	1105.41	57.38	152.03
	120º	850.99	-2.77	186.31	1073.37	55.62	150.61
	150º	827.56	-6.63	186.71	1032.82	52.35	150.58
	180º	836.28	1.04	186.99	1061.23	54.83	148.72
	30º	907.41	-0.94	188.90	1136.45	59.29	153.55
	60º	882.12	0.20	187.35	1111.48	58.79	151.84
1.5	90º	873.14	-2.92	186.99	1096.58	56.23	151.32
	120º	834.36	-4.40	185.38	1054.45	53.69	149.45
	150º	787.35	-9.33	185.38	986.77	49.32	148.83
	180º	787.87	-1.96	185.22	998.59	51.28	146.76

3.2 Effect of Texturing Area

Based on table 6, Cavitation has a significant impact on journal bearing performance, with texture ratio 0.5 at all ε. Journal bearings' maximum pressure and load bearing capacity have increased. Based on table 7, Cavitation has a significant impact on journal bearing performance, with texture ratio 1 at all ε. Journal bearings' maximum pressure and load bearing capacity have increased.

Table 6
Simulation of journal bearing with d/h: 0.5 on ε: 0.2, ε: 0.5 and ε: 0.8

ε	ϑ	without cavitation			with cavitation		
		P_{max} (kPa)	W (kN)	F (N)	P_{max} (kPa)	W (kN)	F (N)
	30º	88.52	0.12	71.65	103.42	1.88	76.99
	60º	92.41	0.55	71.66	107.23	2.25	76.99
0.2	90º	98.02	1.33	71.51	112.39	2.83	76.90
	120º	111.17	2.63	71.16	126.25	3.76	76.67
	150º	109.41	4.21	70.46	122.75	4.73	76.16
	180º	98.72	5.44	69.20	110.22	5.93	74.93
	30º	257.95	-0.70	101.17	328.53	20.63	95.90
	60º	254.86	-1.26	101.09	324.95	19.98	95.72
0.5	90º	252.13	-1.87	101.22	321.10	19.38	95.66
	120º	252.56	-1.60	101.00	317.98	19.26	95.50
	150º	271.99	-0.10	100.73	342.90	20.13	95.42
	180º	248.63	2.54	99.81	315.38	20.67	93.89
	30º	910.73	-0.38	189.20	1140.55	60.00	153.95
	60º	890.07	1.40	188.03	1120.85	60.26	152.69
0.8	90º	889.76	-0.82	188.19	1115.94	58.75	152.80
	120º	871.95	-0.71	187.36	1096.76	57.96	151.87
	150º	874.68	-3.38	188.11	1088.28	56.06	152.38
	180º	871.60	3.44	188.18	1119.99	58.58	150.47

Table 7
Simulation of journal bearing with d/h: 1 on ε: 0.2, ε: 0.5 and ε: 0.8

ε	ϑ	without cavitation			with cavitation		
		P_{max} (kPa)	W (kN)	F (N)	P_{max} (kPa)	W (kN)	F (N)
0.2	30°	86.24	-0.30	71.61	100.77	1.40	76.88
	60°	87.80	-0.22	71.58	101.86	1.45	76.84
	90°	91.34	0.31	71.40	104.45	1.79	76.69
	120°	103.51	1.52	71.05	116.88	2.58	76.41
	150°	102.83	3.18	70.36	114.75	3.64	75.95
	180°	92.57	4.62	69.12	102.41	4.82	74.80
0.5	30°	254.90	-1.23	101.02	324.93	20.04	95.70
	60°	248.30	-2.28	100.81	317.21	18.83	95.29
	90°	241.29	-3.36	100.81	308.12	17.69	95.03
	120°	297.25	-3.45	100.54	298.74	17.14	94.69
	150°	257.48	-1.95	100.23	320.44	17.86	94.58
	180°	234.67	1.24	99.31	294.92	18.65	93.23
0.8	30°	908.90	-0.69	189.04	1138.35	59.62	153.74
	60°	885.67	0.74	187.66	1115.80	59.47	152.26
	90°	880.57	-1.98	187.55	1105.41	57.38	152.03
	120°	850.99	-2.77	186.31	1073.37	55.62	150.61
	150°	827.56	-6.63	186.71	1032.82	52.35	150.58
	180°	836.28	1.04	186.99	1061.23	54.83	148.72

Based on table 8, Cavitation has a significant impact on journal bearing performance, with texture ratio 1.5 at all ε. Journal bearings' maximum pressure and load bearing capacity have increased.

Table 8
Simulation of journal bearing with d/h: 1.5 on ε: 0.2, ε: 0.5 and ε: 0.8

ε	ϑ	without cavitation			with cavitation		
		P_{max} (kPa)	W (kN)	F (N)	P_{max} (kPa)	W (kN)	F (N)
0.2	30°	84.05	-0.70	71.51	98.45	1.05	76.78
	60°	83.25	-0.99	71.38	97.02	0.73	76.59
	90°	84.19	-0.76	71.11	96.78	0.78	76.32
	120°	93.76	0.19	70.70	106.35	1.39	75.97
	150°	92.58	1.69	69.97	104.06	2.25	75.42
	180°	84.05	3.09	68.72	92.78	3.08	74.44
0.5	30°	252.58	-1.63	100.88	322.22	19.59	95.50
	60°	243.28	-3.07	100.51	311.41	17.96	94.88
	90°	232.69	-4.54	100.36	298.30	16.42	94.40
	120°	224.11	-4.99	99.97	283.50	15.51	93.90
	150°	240.09	-3.75	99.61	298.80	15.97	93.63
	180°	219.87	-0.52	98.30	276.50	16.74	92.25
0.8	30°	907.41	-0.94	188.90	1136.45	59.29	153.55
	60°	882.12	0.20	187.35	1111.48	58.79	151.84
	90°	873.14	-2.92	186.99	1096.58	56.23	151.32
	120°	834.36	-4.40	185.38	1054.45	53.69	149.45
	150°	787.35	-9.33	185.38	986.77	49.32	148.83
	180°	787.87	-1.96	185.22	998.59	51.28	146.76

3.3 Tribology Performance

Graph (see Figure 8) comparing pressure distribution journaling bearings without and with cavitation ε = 0.2, ratio D/h_{min} = 1.0 and texture (a) *smooth*, (b) ϑ = 30º, (c) ϑ = 60º, (d) ϑ = 90º, (e) ϑ = 120º, (f) ϑ = 150º, (g) ϑ = 180º

(a)

(b)

(c)
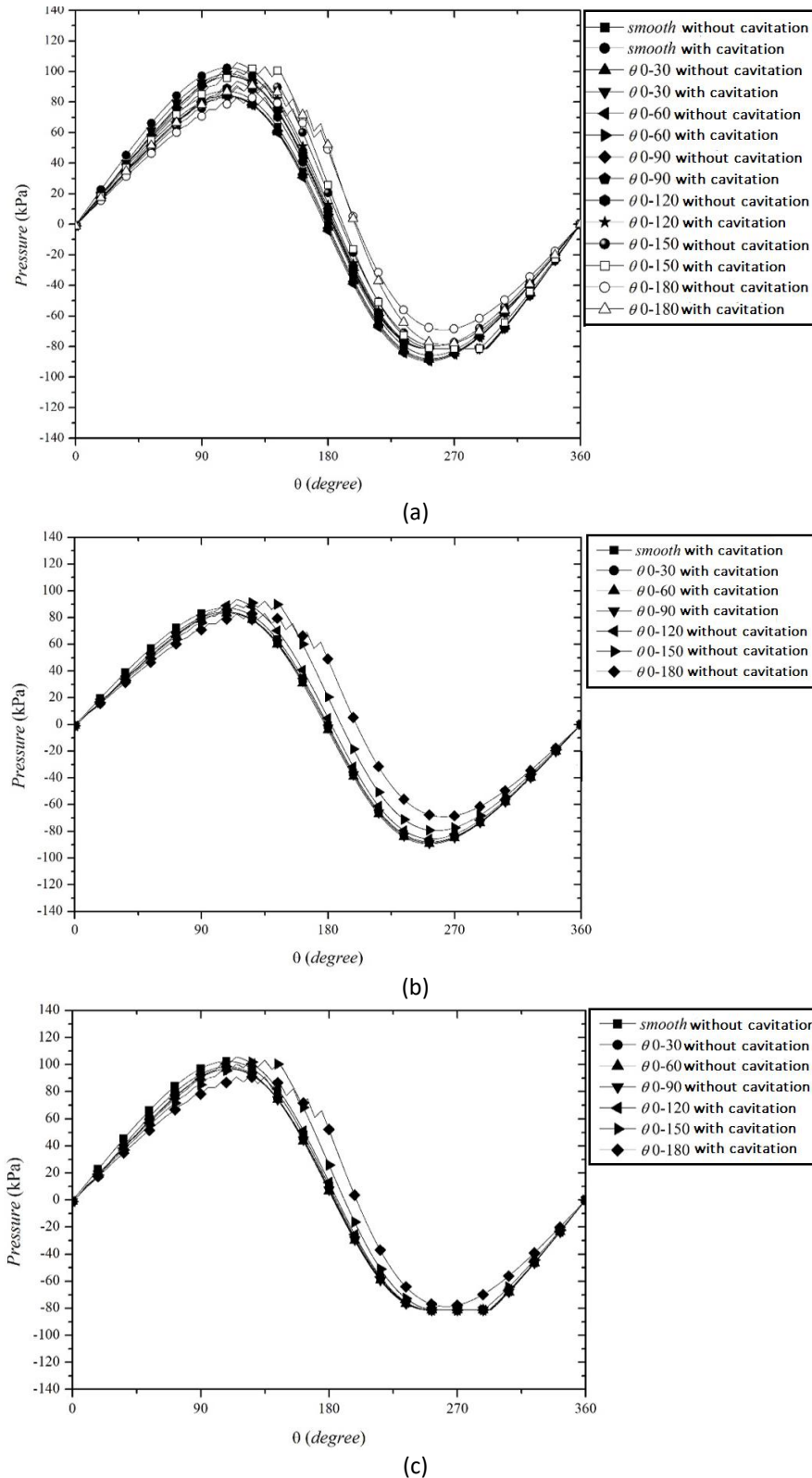
Fig. 8. Graphic pressure ε = 0.2, ratio D/h_{min} = 1.0

The influence of cavitation has a large effect on the performance of journal bearings with ε = 0.2, ε = 0.5, ε = 0.8 in all texture ratios. Evidenced by the increased maximum pressure and load carrying capacity of the journal bearing.

Where in the journal bearing simulation with cavitation, when the hydrodynamic pressure has passed below the cavitation pressure, the journal bearing will lose its hydrodynamic pressure due to the change in the lubrication fluid phase from liquid to vapor in the divergent region. It is characterized by the presence of a straight line on the diverging geometry of the journal bearing. However, the cavitation will disappear and the hydrodynamic pressure will gradually rise again as it approaches the inlet area. Frictional force in the simulation with cavitation also decreased compared to the simulation without cavitation.

4. Conclusion

Based on the results of the research that has been done, several conclusions can be drawn as follows:

The effect of modeling without cavitation and with cavitation on texturing and no-slip boundary conditions has a major influence on the lubrication performance of journal bearings. The maximum hydrodynamic pressure and load carrying capacity that can be supported by journal bearings have increased quite rapidly. However, modeling with cavitation can also increase friction at low eccentricities, namely ε = 0.2, while at high eccentricities, namely ε = 0.5 and ε = 0.8, modeling with cavitation can reduce friction on journal bearings.

The effect of modeling without cavitation and with cavitation on texturing and the slip boundary conditions in the gaps between textured surfaces (partial slip) has a great influence on the lubrication performance of journal bearings. The maximum hydrodynamic pressure and load carrying capacity that can be supported by journal bearings have increased quite rapidly. However, modeling with cavitation can also increase the frictional force at low eccentricity, namely ε = 0.2, while at high eccentricity, namely ε = 0.5 and ε = 0.8, modeling with cavitation can reduce the frictional force on the journal bearing.

The effect of modeling without cavitation and with cavitation on textured and slip boundary conditions in the gaps and all textured surfaces (full slip) has a great influence on the lubrication performance of journal bearings. The maximum hydrodynamic pressure and load carrying capacity that can be supported by journal bearings have increased quite rapidly. However, modeling with cavitation can also increase friction at low eccentricities, namely ε = 0.2, while at high eccentricities, namely ε = 0.5 and ε = 0.8, modeling with cavitation can reduce friction on journal bearings.

References
[1] Hory, "Hydrodinamic Lubrication," *October*, 2006.
[2] Rasep, Zuraidah, Muhammad Noor Afiq Witri Muhammad Yazid, Syahrullail Samion, and Nor Azwadi Che Sidik. "Potential of RBD Palm Oil as a Lubricant in Textured Journal Bearing using CFD with Consideration of Cavitation and Conjugate Heat Transfer." *CFD Letters* 14, no. 2 (2022): 98-110. https://doi.org/10.37934/cfdl.14.2.98110
[3] Syafaat, Imam, Luky Rika Sari, Muchammad Muchammad, Mohammad Tauviqirrahman, Eflita Yohana, Jamari Jamari, and Budi Setiyana. "Numerical Study of Comparison of Thrust Bearing Slip-No Slip Condition on Acoustic Performance." *CFD Letters* 15, no. 9 (2023): 1-17. https://doi.org/10.37934/cfdl.15.9.117
[4] R. C. Juvinall, *Fundamentals of Machine Component Design Fifth Edition*. John Wiley & Sons, Inc., 2012.
[5] Bayada, Guy, and Marie-Hélène Meurisse. "Impact of the cavitation model on the theoretical performance of heterogeneous slip/no-slip engineered contacts in hydrodynamic conditions." *Proceedings of the Institution of*

Mechanical Engineers, Part J: Journal of Engineering Tribology 223, no. 3 (2009): 371-381. https://doi.org/10.1243/13506501JET476

[6] Samanta, Pranab, S. Pradhan, and N. C. Murmu. "Thermal Analysis of Textured Journal Bearing Using Computational Fluid Dynamic Technique." *International Journal of Engineering Research & Technology (IJERT) Vol* 2: 2378-2383.

[7] Androva, Althesa, Muhammad Tuviqirrahman, Nazaruddin Sinaga, Muhammad Khafidh, and Muhammad Sagaf. "Analysis of hydrophobic coating on load carrying capacity of journal bearing considering turbulence effect using CFD FSI method." In *AIP Conference Proceedings*, vol. 2706, no. 1. AIP Publishing, 2023. https://doi.org/10.1063/5.0120603

[8] Versteeg, Henk Kaarle, and Weeratunge Malalasekera. *An introduction to computational fluid dynamics: the finite volume method*. Pearson education, 2007.

[9] J.H.Ferziger and M.Peric, *Computational Methods for Fluid Dynamics*, Third, Rev. Stanford: Springer.

[10] Gropper, Daniel, Ling Wang, and Terry J. Harvey. "Hydrodynamic lubrication of textured surfaces: A review of modeling techniques and key findings." *Tribology international* 94 (2016): 509-529. https://doi.org/10.1016/j.triboint.2015.10.009

[11] Tauviqirrahman, Mohammad, Paryanto Paryanto, Harry Indrawan, Nur Cahyo, Arion Simaremare, and Siti Aisyah. "Optimal Design of Lubricated Journal Bearing Under Surface Roughness Arrangement." In *2019 International Conference on Technologies and Policies in Electric Power & Energy*, pp. 1-5. IEEE, 2019. https://doi.org/10.1109/IEEECONF48524.2019.9102566

[12] Tauviqirrahman, Mohammad, J. Jamari, Muhammad Bagir, Wahyu Caesarendra, and P. Paryanto. "Elastohydrodynamic behavior analysis on water-lubricated journal bearing: A study of acoustic and tribological performance based on CFD-FSI approach." *Journal of the Brazilian Society of Mechanical Sciences and Engineering* 44 (2022): 1-19. https://doi.org/10.1007/s40430-021-03314-9

[13] Navier, Claude. *Mémoire sur les lois du mouvement des fluides*. éditeur inconnu, 1822.

[14] Spikes, Hugh, and Steve Granick. "Equation for slip of simple liquids at smooth solid surfaces." *Langmuir* 19, no. 12 (2003): 5065-5071. https://doi.org/10.1021/la034123j

[15] M. Sagaf, N. Sinaga, M. Tauviqirrahman, M. Khafidh, and A. Androva, "Analysis of the journal bearing performance considering artificial surface roughness and cavitation using CFD FSI method," *AIP Conf. Proc.*, vol. 2706, no. May, 2023, doi: 10.1063/5.0120464. https://doi.org/10.1063/5.0120464

[16] Shi, Xi, and Ting Ni. "Effects of groove textures on fully lubricated sliding with cavitation." *Tribology International* 44, no. 12 (2011): 2022-2028. https://doi.org/10.1016/j.triboint.2011.08.018

[17] Wang, Li-li, and Chang-hou Lu. "Numerical analysis of spiral oil wedge sleeve bearing including cavitation and wall slip effects." *Lubrication science* 27, no. 3 (2015): 193-207. https://doi.org/10.1002/ls.1267

[18] Dobrica, M. B., M. Fillon, M. D. Pascovici, and T. Cicone. "Optimizing surface texture for hydrodynamic lubricated contacts using a mass-conserving numerical approach." *Proceedings of the Institution of Mechanical Engineers, Part J: Journal of Engineering Tribology* 224, no. 8 (2010): 737-750. https://doi.org/10.1243/13506501JET673

[19] Sauer, Jürgen, and G. H. Schnerr. "Development of a new cavitation model based on bubble dynamics." *ZAMM-Journal of Applied Mathematics and Mechanics/Zeitschrift für Angewandte Mathematik und Mechanik* 81, no. S3 S3 (2001): 561-562. https://doi.org/10.1002/zamm.20010811559

[20] Zwart, Philip J., Andrew G. Gerber, and Thabet Belamri. "A two-phase flow model for predicting cavitation dynamics." In *Fifth international conference on multiphase flow, Yokohama, Japan*, vol. 152. 2004.

[21] Cupillard, Samuel, Sergei Glavatskih, and M. J. Cervantes. "Computational fluid dynamics analysis of a journal bearing with surface texturing." *Proceedings of the Institution of Mechanical Engineers, Part J: Journal of Engineering Tribology* 222, no. 2 (2008): 97-107. https://doi.org/10.1243/13506501JET319

[22] Hamrock, Bernard J., Steven R. Schmid, and Bo O. Jacobson. *Fundamentals of fluid film lubrication*. CRC press, 2004. https://doi.org/10.1201/9780203021187